ICAS 2020 SHANGHAI
International Council of the Aeronautical Sciences
32nd Congress of the International Council of the Aeronautical Sciences
September 6-10, 2021
Pudong Shangri-La, Shanghai, China

Methodology for Obtaining an Optimized Baffled Airfoil for an Inflatable Wing

Sohrab R. Mistri[1], Rajkumar S. Pant[1], Chandra Sekher Yerramalli[1] and Anirban Guha[2]

[1]Department of Aerospace Engineering, Indian Institute of Technology Bombay
[2]Department of Mechanical Engineering, Indian Institute of Technology Bombay

Abstract

Although many attempts have been made to manufacture inflatable wings, a standardized method to generate and communicate the geometric details of an inflatable airfoil is not found in the literature. This paper attempts to fill this lacuna. The paper begins with a brief introduction to inflatable wing technologies and discusses a few milestones of the technology. Further, the paper predicts the shape of a single compartment of an inflatable airfoil. The paper then formally introduces a geometric method to convert a conventional airfoil into an inflatable airfoil, with equally spaced baffles. A preliminary attempt to reduce the deviation of the inflatable airfoil from its original airfoil is undertaken. The angle of the first baffle is varied to reduce the Area Change Ratio (ACR), a term defined to quantify deviation of the inflated airfoil from the original airfoil. Based on this study, a standardized nomenclature for inflatable airfoils is proposed which can be used by researchers in this field.

Keywords: Hand Launched UAVs, Inflatable wings, Baffled wings, Shape Optimization

1. Introduction

Inflatable wings are useful where storage space is a constraint. A typical example of such a scenario is an on-field soldier who needs to deploy a backpack carry-able Unmanned Aerial Vehicle (UAV) for surveillance. Inflatable wings use air beams as their structural backbone. These air beams together form the airfoil shape. The air beams can be circular in shape while joined by an open cell foam structure, or the airfoil itself can be built of multiple compartments along the wingspan (Figure 1). These systems are either inflated in flight or on the ground. A few benchmark projects related to inflatable wings are listed below.

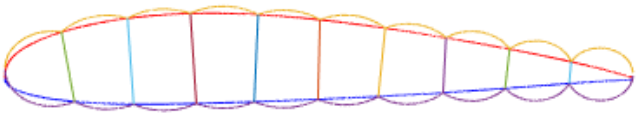

Figure 1 – Typical Inflatable Airfoil

McDaniel's glider (1930) is one of the earliest records of inflatable wings [1]. It consisted of tubular spars as the structural element. The inflatable wings were warped to establish roll control. Later in 1956, the Goodyear *Inflatoplane* was designed with the intention of recovering surviving pilots behind enemy lines [2] [3]. In 1970, *Apteron*, the first UAV utilizing inflatable wing technology was designed [4]. The aim was to design an aircraft that can be stored in a low form factor and can be launched easily in remote locations. In 2002, the *I-2000* was launched, which was a conventional UAV designed by the NASA Dryden Flight Research Centre. The purpose of *I-2000* was to study the flight characteristics of inflatable wings compared to fixed wings [5]. In 2004, the *BIG BLUE* UAV was designed at University of Kentucky to check the feasibility of UV cured/hardened wings [6].

An in-depth literature review reveals that the research on inflatable wings can be categorized into four major sub-disciplines, viz., Structures, Materials, Aerodynamics and Morphing, and sub systems such as the inflation mechanism. Jun-Tao et al. [7] have covered the theoretical concepts for structural strength of air beams. Walker et al. [8] and Murray et al. [5] have conducted practical load testing of an inflatable wing. Breuer et al. [9] have introduced the concept of Tenacity. Metal wires run along the air beams providing addition support hence reducing the requirement of pressure from the inflation system. With regards to research in the field of materials, a curable wing is a sought-after attribute.

Cadogan et al. [10] have expanded on various curing techniques such as thermally cured thermoset composites, ultra-violet cured composites, inflation gas reaction composites and second order transition change and shape memory polymer (SMP) composites. Haight et al. [11] have performed experiments in curing wings using an UV-LED blanket. Another successful deployment of rigid inflatable wing is the *BIG BLUE* project [6]. In the field of aerodynamics, Jun-Tao et al. [7] have conducted practical testing on NACA 0012 in its inflatable wing form. LeBeau et al. [12] have performed a numerical comparison of flow over bumpy inflatable airfoils.

This review of papers shows that while many attempts have been made at fabricating inflatable airfoils, a standardized approach to generate and communicate the geometric details of the inflatable airfoil has not been reported in the literature. A standardized approach to create and communicate the geometric details of an inflatable airfoil is necessary as it would facilitate collaborations and validations across the scientific community.

This paper begins with the geometric shape identification of a single air beam that comprises of two baffles which result in two bulging fabric members at the top and bottom. The paper further discusses the inflatable airfoil generation process for both types of inflatable airfoils and attempts to reduce the geometric deviation of the inflatable airfoils from their original airfoil. Further, an inflatable airfoil specification procedure is laid out to aid researchers to accurately communicate the geometry of the inflatable wing.

2. Inflated profile identification

The inflated airfoil shape is typically obtained by inflating a fabric cut and stitched in the shape of an airfoil. A methodology to predict the inflated shape of the airfoil is presented in this section. During the inflation process, the upper and lower fabrics of the airfoil will deform to create an outward bulge as well as some stretch in the fabric due to the internal pressure. The outward bulge is assumed to be circular in shape as the internal pressure is constant. In this analysis, the change in length of the fabric is ignored while predicting the shape of the inflated fabric.

The inflatable airfoil can be considered as a series of compartments. This section predicts the shape of these compartments for the specific case of unequal parallel baffles and for the generic case of unequally tilted baffles.

A. Unequally tilted baffles

This section addresses the case of unequal tilted baffles as seen in Figure 2. '*p,q,r,s'* indicate four cutting lines. A geometrical approach to derive the location of the center is implemented.

Consider reorienting Figure 2 such that cutting line '*p*' is horizontal as shown in Figure 4. To keep element 'a' in balance (Figure 4), the horizontal forces, F_x must be equal and opposite. The vertical forces, F_y must be equal in magnitude and have the same direction to sum up to the pressure P acting internally.

This implies that the resultant forces at the two end nodes of element 'p' are equal and mirrored about the perpendicular bisector. Since the fabric cannot resist bending loads, the slope of the fabric or the derivative is F_y/F_x. Hence the centers of the side arcs as seen in Figure 4 are mirrored along the perpendicular bisector.

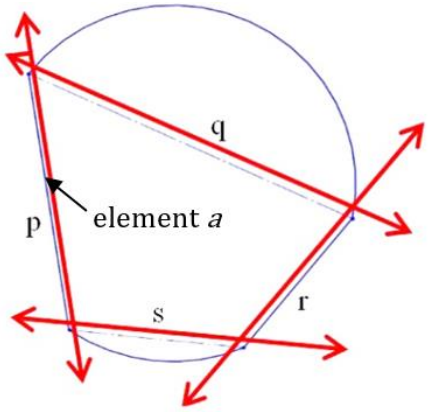

Figure 2 – Unequal tilted baffles

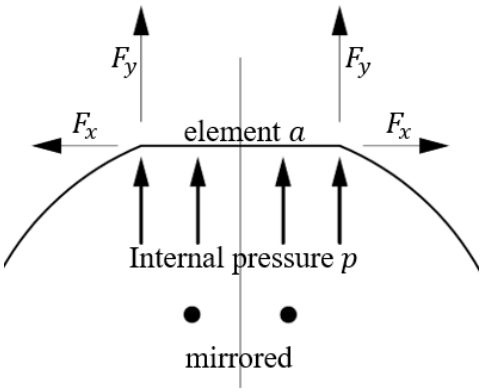

Figure 4 – Unequal baffles
(single baffle view)

The same can be said for both baffles and the other two dotted sides as shown in Figure 3. The only way for the centers of the top and bottom fabrics to be mirrored in all four perpendicular bisectors is for all four perpendicular bisectors to intersect at one point. This point represents the circle center coordinates of the top and bottom fabrics. Thus, each compartment has a circular cross section and can be thought of as an air beam in 3D.

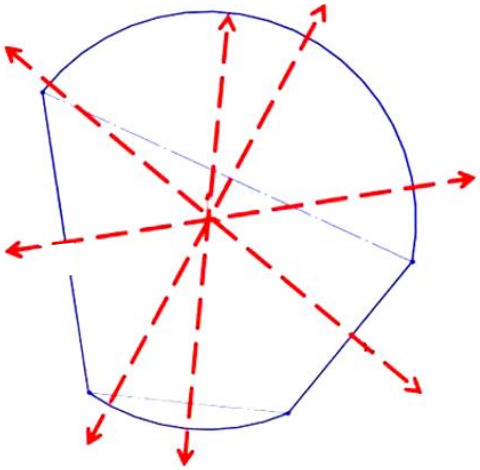

Figure 3 – Tilted unequal baffles

Since each compartment is forming a single circle, the entire structure can be created as a combination of intersecting circles that form the shape of the bumpy airfoil. The points where the circles intersect determine the location of the baffles. The bumps result in deviation of shape from the original airfoil. A parameter to quantify the deviation of the inflatable airfoil to its conventional airfoil is needed. This is introduced as the unitless parameter, Area Change Ratio (ACR) which is defined as the ratio of the change in the area of the inflatable airfoil to the area of the conventional airfoil as seen in equation (1). The area refers to the cross-sectional area of the airfoil as seen.

$$ACR = \frac{\left|Area_{inflatable\ airfoil} - Area_{original\ airfoil}\right|}{Area_{original\ airfoil}} \quad (1)$$

The shape of a single air beam has been derived in this section. The next section elaborates on a method to create an airfoil by joining multiple air beams.

3. Inflatable airfoil generation algorithm

An overview of the algorithm designed to create the baffled airfoil is shown in Figure 5. Although the process for converting a symmetrical airfoil to an inflated baffled airfoil is intuitive, the process for converting an unsymmetrical airfoil is not and requires a formalization of the process. The step-by-step process to convert any airfoil (symmetric or un-symmetric) to a baffled airfoil is explained below.

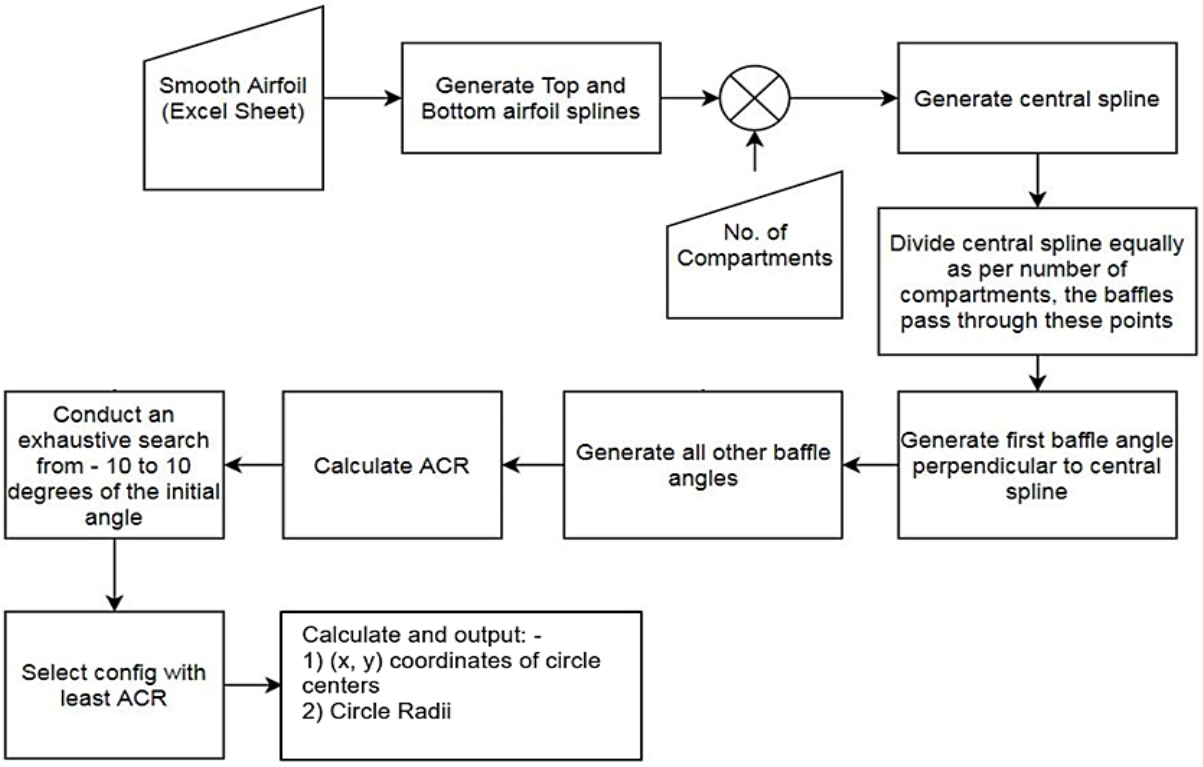

Figure 5 – Flowchart for conversion of conventional to inflatable airfoil

3.1 Inputs

The user needs to give the coordinate points of the smooth airfoil in the form of an excel sheet. The user can also give the NACA 4-digit series number and the code will create the smooth airfoil coordinates itself. Once the smooth airfoil coordinates are given, the user needs to give the number of compartments needed to create the inflatable airfoil.

3.2 Converting inputs to code requirements

First, the coordinates are used to generate the upper and lower splines of the smooth airfoil. The central spline is generated, and the coordinates of the points equally spaced along the x-axis as per given number of compartments are calculated. The baffles will pass through these points on the central spline. For a particular angle of one of the baffles, the angles of all other baffles need to be calculated (through the procedure described in section (3.5) so that the inflatable conforms to the shape of the original airfoil.

3.3 Finding baffle intersection points with the smooth airfoil

One way to calculate the intersection point of the baffle and the airfoil is to solve both simultaneously. However, MATLAB [14] stores the top and bottom airfoils as a piecewise third-degree spline. Hence the equation for the baffle intersection point must be solved simultaneously with each segment of the spline and the derived intersection point would have to be crosschecked to lie within the upper and lower bounds of the concerned spline segment. This would be an iterative procedure. Instead, a binary search algorithm is used to evaluate the coordinates of the intersection points within an accuracy of (10^{-6}) units for 1 unit of chord length.

3.4 Calculating circle center coordinates and radius given three points

The equations illustrated here are used in section 3.5. Let the three available points that the circle passes through be (x_1,y_1), (x_2,y_2), (x_3,y_3). The circle center coordinates (C_x,C_y) and radius 'r' are known.

Substituting the three given coordinates into the equation of a circle and rearranging the terms of the three equations generated in matrix form: -

$$\begin{bmatrix} 2x_1 & 2y_1 & 1 \\ 2x_2 & 2y_2 & 1 \\ 2x_3 & 2y_3 & 1 \end{bmatrix} \begin{bmatrix} C_x \\ C_y \\ r^2 - {C_x}^2 - {C_y}^2 \end{bmatrix} = \begin{bmatrix} -{x_1}^2 - {y_1}^2 \\ -{x_2}^2 - {y_2}^2 \\ -{x_3}^2 - {y_3}^2 \end{bmatrix} \quad (2)$$

The circle center coordinates, and their radii can be calculated by solving Equation (2).

3.5 Calculating subsequent baffles given the first baffle angle

Once the first baffle angle is fixed and the intersection points are found, the subsequent baffle angles can be calculated one after the other. In each step, the left baffle becomes the known and the right baffle angle needs to be calculated. Referring to Figure 6, two circles are drawn, one passes through points $P_1, P_4\ P_2$ as seen in Figure 6 and the other passes through points $P_1, P_4\ P_3$. Equation (2) is used to calculate the radii given the set of 3 points. For all 4 points to pass through the same circle, these radii must be equal. Hence the angle of the second baffle is varied to minimize the difference between the two radii. The process is then repeated for the next air beam.

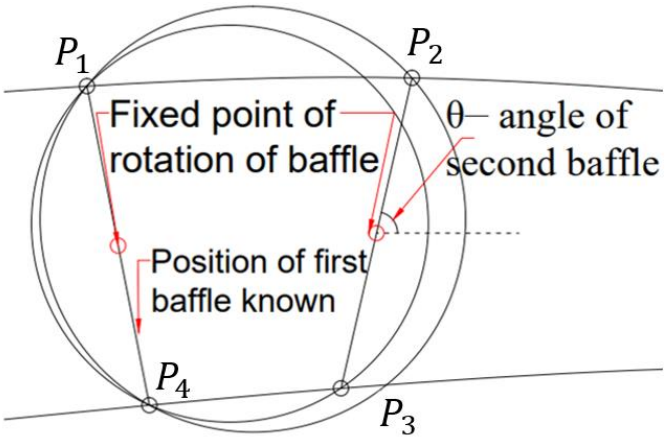

Figure 6 – Calculation of second baffle angle

3.6 Outputs

An example of the output generated for an airfoil with 20 compartments is shown in Figure 7.

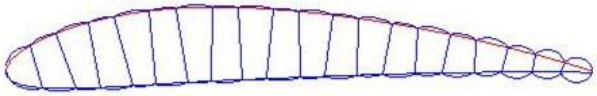

Figure 7 – Bumpy airfoil with 20 compartments

The change in the ACR as the number of compartments increase is shown in Figure 8. The increase in area reduces as the number of compartments increase.

The user can use this information to export into another software for further analysis or use it to calculate the lengths of the fabric needed for the upper and lower bulging fabrics and the baffles during manufacturing.

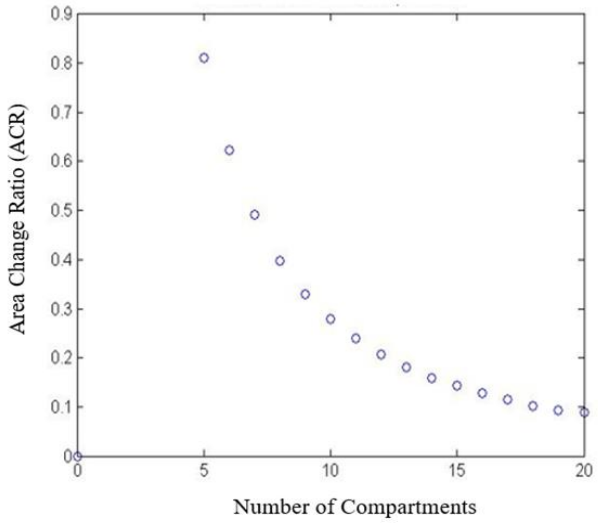

Figure 8 – ACR vs number of compartments

4. ACR Minimization by varying the first baffle angle

For a particular number of baffles, the angle of the first baffle determines the angles of all the subsequent baffles. The ACR is dependent on the angle of the first baffle. An algorithm was developed to minimize the ACR by changing the angle of the first baffle. Figure 9 shows two different configurations for the same baseline specifications (NACA 4318) with eight equally spaced compartments.

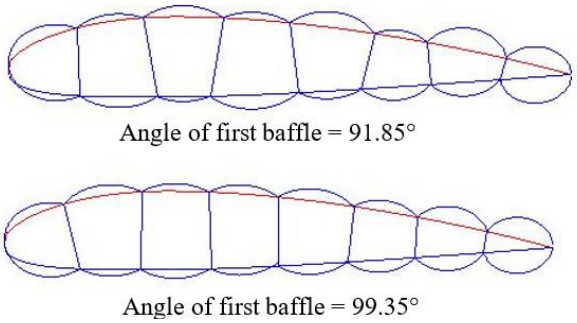

Figure 9 – NACA 4318, 8 compartments, different angle of first baffle

The study of ACR v/s the angle of the first baffle is conducted on two different type of airfoils: - symmetrical and semi-symmetrical. The details of the airfoils are given in Table 1.

Table 1. Cases for which ACR minimization is performed

Case No.	Airfoil	Number of compartments	Type of Airfoil	Airfoil
1	0014	13	Symmetrical	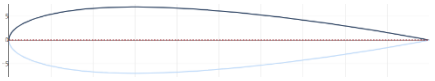
2	4318	13	Semi-symmetrical	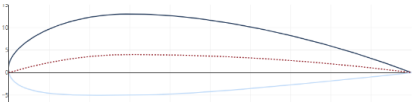

Figure 10 illustrates the effect of changing the angle of the first baffle on ACR for the two different cases. The vertical line indicates the angle of the first baffle that is vertical to the center spline. The same is considered as the initial guess. The ACR is calculated for $\pm 5^{\circ}$ from the initial guess with 0.5° intervals. In the case of the symmetrical airfoil, the optimum angle of the first compartment is the same as the initial guess. However, for the semi-symmetrical case, the same does not coincide. Earlier literature considers an arbitrary first angle as an initial guess. However, Figure 10 indicates that the maximum value of ACR is approximately 4% higher than the optimum ACR for the symmetrical case and approximately 10% higher for the semi-symmetrical case.

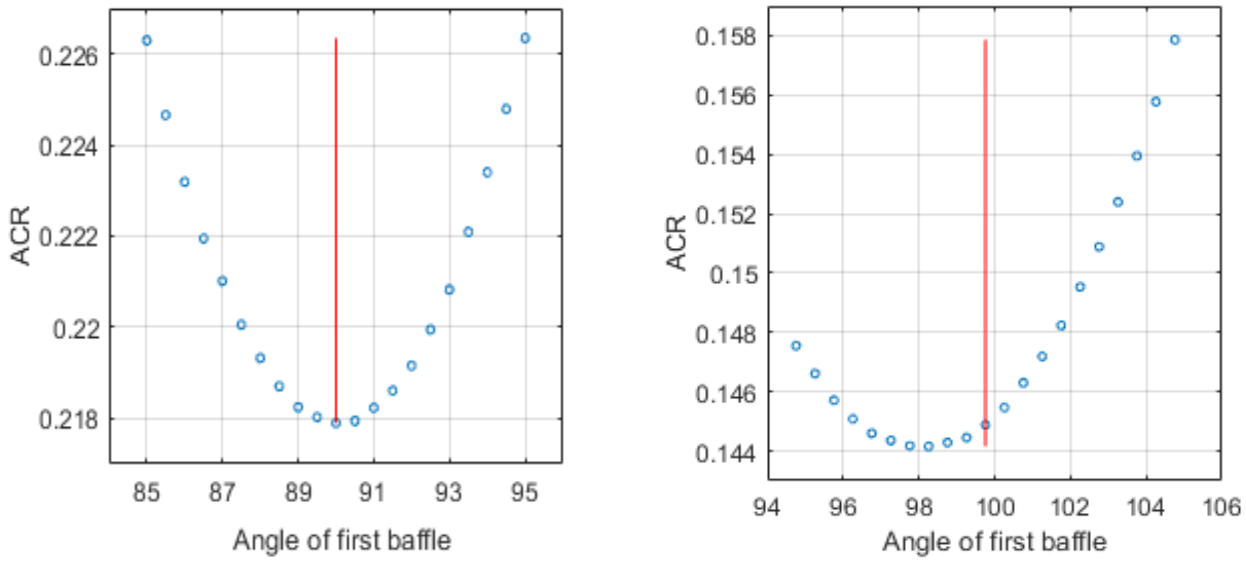

(a) NACA 0014 (b) NACA 4318

Figure 10 – Increase in ACR vs angle of first baffle in degrees

5. Inflatable airfoil specification procedure

A standard procedure for specifying the geometric parameters of inflatable airfoils was not found in literature. This poses as a challenge for cross community validation and research. The number of baffles or compartments have often been specified, however the details of the geometry need to be communicated. It is found that the circle center coordinates and the radii of each compartment fully define the geometries of the inflatable airfoil. The dimensions should be normalized to the original smooth airfoil having a chord of length unity. An inflatable airfoil specification procedure is suggested as seen in Table 2. The same should be mentioned for every inflatable airfoil under consideration.

Table 2 – inflatable airfoil specification procedure

Airfoil Name			Chord of smooth airfoil: 1 unit			
Compartment No.	1	2	3	4	……	N
Cx						
Cy						
r						

Cx is the x-coordinate of circle center, Cy is the y-coordinate of circle center and r is the radius of the compartment. Compartment number ranges from 1 to the max number of compartments. Cx, Cy, r are all standardized to the original airfoil chord length of 1 unit. For example, consider NACA 4318 converted to an inflatable airfoil as seen in Figure 11.

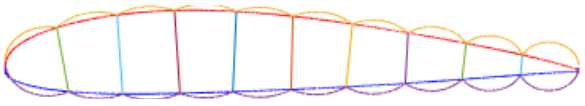

Figure 11 – NACA 4318 converted to an inflatable airfoil of 10 compartments

The same is specified in Table 3 as: -

Table 3 – NACA 4318 converted to inflatable airfoil specification procedure

NACA 4318	Type of inflatable airfoil if any									
	Compartment Numbers.									
	1	2	3	4	5	6	7	8	9	10
Cx	0.075	0.162	0.254	0.347	0.444	0.542	0.642	0.743	0.845	0.948
Cy	0.019	0.032	0.037	0.042	0.039	0.037	0.029	0.024	0.015	0.008
r	0.075	0.094	0.101	0.102	0.097	0.090	0.080	0.070	0.060	0.052

6. Conclusion and future work

This paper formally introduces a method to generate inflatable baffled airfoils which closely match a given conventional airfoil. This has been achieved by placing baffles in the inflated airfoil. A method of predicting the shape of such an inflated baffled airfoil has been deduced and used to reduce the geometric deviation between the inflatable airfoil and original airfoil. A number of parameters have been identified which would be needed to be reported to ensure that a specific inflated airfoil can be duplicated. These parameters include the number of compartments and position of each compartment center. A common method to report these parameters has been proposed.

One important finding was that the angle of any one baffle forced the angles of all other baffles to take up a specific value if the inflated system needs to confirm to the original airfoil. This allowed the difference between areas of the inflated and original airfoils to be minimized by changing the baffle angles. The effect of the number of baffles on this minimization exercise has also been reported. Future work can extend this optimization exercise to arbitrarily placed baffles which may be needed for highly cambered airfoils.

Parameters other than the change in area can be chosen as objective functions in the optimization process. Hence, future work could include choosing parameters that have an impact in a multidisciplinary framework involving structures and aerodynamics. Parameters such as Cl/Cd and section modulus or strength to weight ratio can be used as objective functions. These may show a greater improvement due to the optimization exercise compared to the change in area.

7. Contact Author Email Address

mailto: sohrabmistri@hotmail.com

8. Copyright Statement

9. References

[1] T. McDaniel, "T. M'c Daniel Flying Machine". United States Patent Office Patent 1,905,298, 1933., 25th April 1933.

[2] R. K. Norris and W. J. Pulliam, "Historical Perspective on Inflatable Wing Structures," in 50th AIAA/ASME/ASCE/AHS/ASC Structures, Structural Dynamics, and Materials Conference, Palm Springs, California, 2009, DOI: 10.2514/6.2009-2145.

[3] J. Winchester, The World's Worst Aircraft: From Pioneering Failures to Multimillion Dollar Disasters, Barnes & Noble Books, 2005.

[4] D. Cadogan, W. Graham and T. Smith, "Inflatable and Rigidizable Wing for Unmanned Aerial Vehicles," in 2nd AIAA "Unmanned Unlimited" Conference and Workshop & Exhibit, San Diego, California, 2003, DOI: 10.2514/6.2003-6630.

[5] E. Murray, J. Pahle, S. Thornton, S. Vogus, T. Frackowiak, J. Mello and B. Norton, "Ground and Flight Evaluation of a Small-Scale Inflatable-Winged Aircraft.," in 40th AIAA Aerospace Sciences Meeting & Exhibit, Reno, Nevada, 2002, DOI: 10.2514/6.2002-820.

[6] A. Simpson, O. Rawashdeh, S. Smith, J. Jacob, W. Smith and J. Lumpp, "BIG BLUE: high-altitude UAV demonstrator of Mars airplane technology," in 2005 IEEE Aerospace Conference, Big Sky, Montana, USA, 2005, DOI: 10.1109/AERO.2005.1559753.

[7] Z. Jun-Tao, H. Zhong-xi and C. L.-l. Guo Zheng, "Analysis and Flight Test for Small Inflatable," World Academy of Science, Engineering and Technology, vol. 6, no. 9, pp. 1934-1939, 2012, DOI: 10.5281/zenodo.1329184.

[8] A. Scott J.I.Walker, "Initial performance assessment of hybrid inflatable structures," Acta Astronautica, vol. 68, no. 7-8, pp. 1185-1192, 2011, DOI: 10.1016/j.actaastro.2010.10.009.

[9] J. Breuer, W. Ockels and R. H. Luchsinger, "An inflatable wing using the principle of Tensairity," in 48th AIAA/ASME/ASCE/AHS/ASC Structures, Structural Dynamics, and Materials Conference, Honolulu, Hawaii, 2007, DOI: 10.2514/6.2007-2117.

[10] D. P. Cadogan and S. E. Scarborough, "Rigidizable materials for use in gossamer space inflatable structures," in 19th AIAA Applied Aerodynamics Conference, Anaheim, California, U.S.A., 2001, DOI: 10.2514/6.2001-1417.

[11] A. H. Haight, R. Allred, L. Harrah, P. McElroy, S. Scarborough and T. Smith, "Design and Fabrication of Light Rigidizable Inflatable Wings," in 47th AIAA/ASME/ASCE/AHS/ASC Structures, Structural Dynamics, and Materials Conference, Newport, Rhode Island, 2006, DOI: 10.2514/6.2006-1695.

[12] R. LeBeau, D. Reasor, T. Gilliam, A. Schloemer, T. Hauser and T. Johansen, "Numerical Comparison of Flow over Bumpy Inflatable Airfoils," in 47th AIAA Aerospace Sciences Meeting including The New Horizons Forum and Aerospace Exposition, Orlando, Florida, 2009, DOI: 10.2514/6.2009-1306.

[13] S. R. Kancherla, C. R. Dusane, S. R. Mistri and R. S. Pant, "Analytical Modelling of Baffled Inflatable Wing for Failure Prediction," in AIAA Aviation 2019 Forum, Dallas, Texas, 2019, DOI: 10.2514/6.2019-3366.

[14] The MathWorks Inc., MATLAB. (2020). version 9.9.0.1467703 (R2020b), Natick, Massachusetts.